Eur. Phys. J. B **18**, 247–255 (2000)

THE EUROPEAN PHYSICAL JOURNAL B

EDP Sciences

Galvanomagnetic properties of disordered Mn semi-Heusler phases with Anderson localisation

J. Pierre[1,a], K. Kaczmarska[2], and J. Tobola[3]

[1] Laboratoire L. Néel, CNRS, BP 166 X, 38042 Grenoble, France
[2] Institute of Physics, University of Silesia, Uniwersytecka 4, 40007 Katowice, Poland
[3] Faculty of Physics and Nuclear Techniques, al. Mickiewicza, 30058 Krakow, Poland

Received 31 May 2000

Abstract. The Anderson localisation has been observed in Heusler-type solid solutions where Mn replaces Ti or V in NiTiSb or CoVSb compounds respectively, due to the atomic and magnetic disorders. The magnetoresistance, Hall effect, thermopower and electron spin resonance of these solutions are investigated. Strong anomalies appear for the concentration range where a carrier localisation occurs; the mobility of carriers is strongly reduced, the magnetoresistance scales with the resistivity and the susceptibility of solid solutions.

PACS. 71.55.Jv Disordered structures; amorphous and glassy solids – 72.15.Gd Galvanomagnetic and other magnetotransport effects – 72.15.Jf Thermoelectric and thermomagnetic effects

1 Introduction

Semi-Heusler phases are ternary compounds involving two different transition metals and one *sp* element like Sn, Sb or Bi. They are rather well known since the discovery of the half-metallic character in the ferromagnetic NiMnSb and PtMnSb phases [1,2]. They are built from four interpenetrating fcc sublattices, one of them being unoccupied. Due to this void, the overlap of d wavefunctions is small, giving rise to narrow bands and to the presence of gaps in the energy spectrum. The properties of these phases have been much studied recently, particularly their magnetic, transport properties [3,4] and electronic structures [5,6]. Semiconductors, semi-metals, normal Pauli metals, weak ferromagnets, antiferromagnets, as well as strong half metallic ferromagnets exist in this series, giving rise to a model system for studying the onset of magnetism and the modifications of transport properties as function of the electronic structure. In addition, these phases may have important applications, due to the giant Kerr effect (PtMnSb) [7], the half metallic character (PtMnSb, NiMnSb) [8], the very large thermopower (ZrNiSn, HfNiSn [3,9] and other doped semiconductors [10]).

In a recent work [11], the properties of solid solutions between normal or weakly ferromagnetic metals and Mn-based strongly ferromagnetic metals have been studied, namely the $NiTi_{1-x}Mn_xSb$ and $CoV_{1-x}Mn_xSb$ solutions. Surprisingly, solid solutions with about 35% of Mn show a semiconducting-like resistivity, which cannot be explained by the presence of a normal energy gap. The magnetic and transport properties have been analyzed within the framework of the Anderson localisation due to the atomic and magnetic disorders as follows.

For a low Mn concentration, the conduction is metallic, the Mn $3d$ levels being buried well below the Fermi level [11] and the magnetic interactions between them are weak. Near $x = 0.35$, the Mn $3d$ levels begin to overlap and to reach the Fermi level, there is a strong scattering of carriers due to the charge difference between Mn and Ti or V, and to the disordered magnetic moments of Mn atoms, giving rise to the localisation of carriers; the resistivity becomes three orders of magnitude larger than in the starting compounds and is semiconducting-like (Fig. 1). Semiconducting-like means that the resistivity decreases with temperature, and has a magnitude which is larger than the Yoffé-Regel-Mott limit for metallic conductivity, corresponding to a mean free path reduced to one interatomic distance. For $x > 0.5$, extended Mn energy bands are formed and the resistivity returns to a metallic character; a percolation threshold for magnetic interactions between Mn atoms is reached and the ferromagnetic interactions rapidly increase.

The density of states (DOS) has been calculated for solid solutions [6,11] by the Kohn-Korringa-Rostoker (KKR) method using Coherent Potential Approximation [12]. The partial densities for each component are then obtained, knowing that they represent the partial DOS assuming a mean surrounding potential; the method does not allow to take a full account of the disorder leading to localisation phenomena, but gives a valuable knowledge of the electron states for the various components.

[a] e-mail: jacques.Pierre@polycnrs-gre.fr

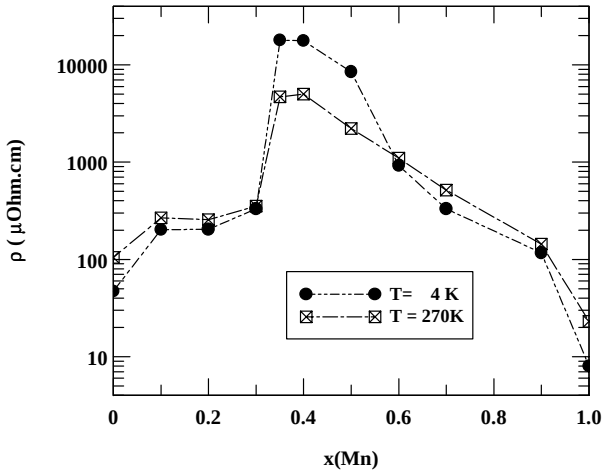

Fig. 1. Resistivity at 4 K and 270 K in the $NiTi_{1-x}Mn_xSb$ series.

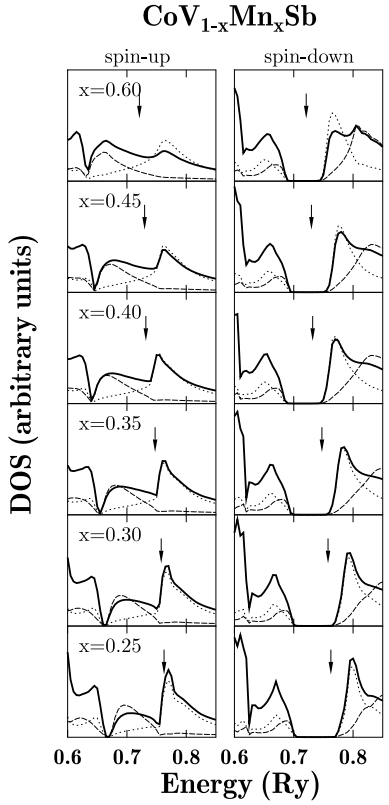

Fig. 2. KKR-CPA spin polarized density of states for some $CoV_{1-x}Mn_xSb$ solutions in the vicinity of E_F (see also Ref. [11]). Total as well as V and Mn DOS contributions are drawn as thick solid, dotted and dashed lines respectively. The Fermi level is marked by a vertical arrow.

The total and partial DOS around the Fermi level E_F are given in Figure 2 for some $CoV_{1-x}Mn_xSb$ solutions. The down spin density at E_F is vanishing for solutions in this concentration range, allowing to classify them as half metals [1,2]. In this range of x, the magnetization increases at the rate of 1 μ_B by added electron, as it should be for half metallic solutions [11]. For low Mn concentrations, there is a density rising with energy near E_F, coming mainly from V $3d$ states, whereas for large Mn concentrations, the DOS is decreasing around E_F, due to Mn and Co decreasing DOS. For the Mn concentrations ($x = 0.35 \div 0.45$) corresponding to localised carriers, there is a minimum in the density of states in the vicinity of the Fermi level, arising mainly from the decreasing DOS from Mn and Co $3d$ shells and increasing DOS coming from V. This, together with the atomic and magnetic disorders, may explain the localisation of current carriers. A similar behaviour is observed in the $NiTi_{1-x}Mn_xSb$ series.

In this paper, we bring additional data concerning the galvanomagnetic properties of these solutions (magnetoresistance, Hall effect, thermopower) and the electron spin resonance in some phases, which will complement the description of the localisation mechanism. The reader is referred to the reference [11] for the structural, magnetic, resistivity data and the band structure calculations concerning these solutions.

2 Magnetoresistance

The resistivity was measured by the classical AC current four probes method; the magnetoresistance, measured for fields up to 8 T, is defined as:

$$MR(H) = [\rho(H) - \rho(0)]/\rho(0).$$

If not specified, the longitudinal (LG) magnetoresistance is given.

2.1 $NiTi_{1-x}Mn_xSb$ solutions

The magnetoresistance (MR) of the NiTiSb Pauli metal is positive, with a magnitude decreasing with temperature as expected for a cyclotron contribution. At 10 K, its value reaches 1.7% under 4 T and 5% under 8 T. For the NiMnSb half metallic ferromagnet, the MR is also positive at low temperatures, the transverse MR being larger than the longitudinal one [13]; the LG-MR reaches 2.3% under 4 T at 10 K, it decreases rapidly with temperature and changes its sign above 100 K, where a negative spin disorder contribution becomes dominant. The spin disorder term should be very weak at low temperature in the half metallic regime, as incoherent spin flip processes are inelastic and do not contribute [13], and as the spin wave contribution is low due to the high Curie point (T_C = 730 K) and high spin wave stiffness. Conversely the spin disorder term overcomes the cyclotron term when NiMnSb becomes a normal metal above 80 K, due to the reduction of the ferromagnetic band splitting.

For the $NiTi_{1-x}Mn_xSb$ solid solutions, we recall that for x(Mn) ≤ 0.45 the ordering points are very low (below 15 K) and the ground state is a spin glass (Kaczmarska *et al.*, to be published). Conversely the solutions turn ferromagnetic for $x \geq 0.5$, and the Curie point T_C then increases very rapidly with x. As said in the introduction, the resistivity turns semiconducting-like in the range $0.35 < x < 0.5$.

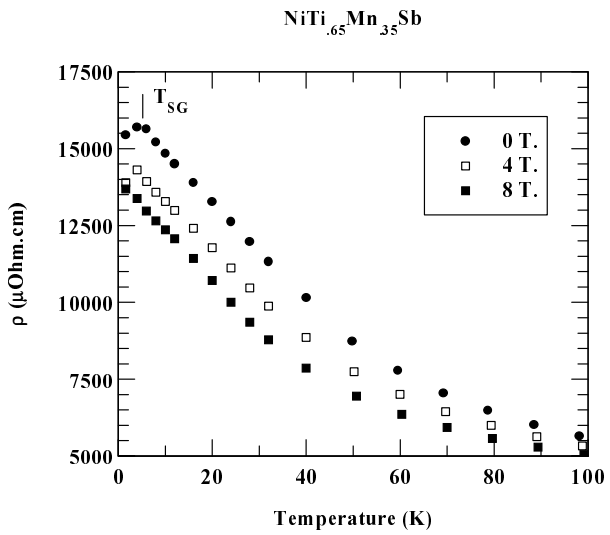

Fig. 3. Resistivity under 0, 4 and 8 T for $NiTi_{0.65}Mn_{0.35}Sb$. TSG is the spin glass temperature.

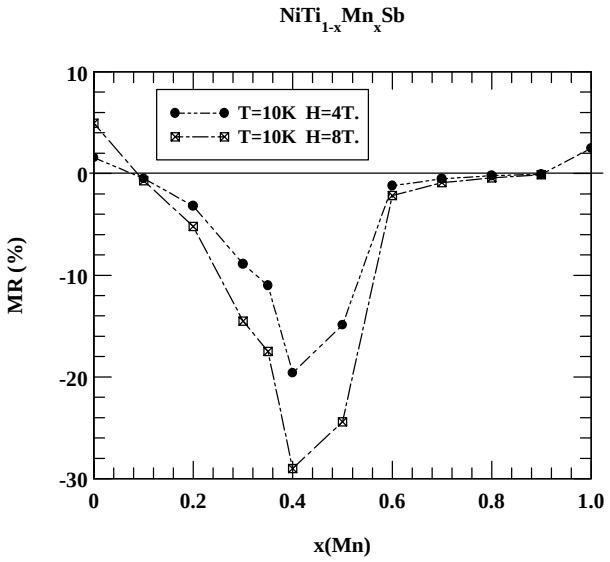

Fig. 4. Magnetoresistance amplitudes under 4 T and 8 T in the $NiTi_{1-x}Mn_xSb$ series.

Starting with low Mn concentrations ($0.2 \div 0.3$), the resistivity shows a metallic behaviour with a upturn below 50 K which was interpreted as a Kondo-like behaviour [11]. The MR is negative and the stronger, the lower is the temperature; for $x = 0.3$, it reaches -14.5% under 8 T at 10 K. The low temperature resistivity upturn disappears for $H > 2$ T, thus for higher fields the resistivity steadily increases with temperature. The magnitude of the MR follows more or less the temperature dependence of the susceptibility, being largest near 10 K. However, it is more or less proportional to H^2 for temperatures above 30 K and becomes rather linear with the field at 2 K (in the spin glass region). The most plausible interpretation is that spin fluctuations are suppressed under field.

For x(Mn) $= 0.35 \div 0.45$, the resistivity enters in a localisation regime, it may be described in a medium temperature range (typically 20–120 K) by $\rho = \rho_{\mathrm{VRH}}\, exp(T_0/T)^p$, where T_0 is the Mott temperature and $p = 0.25$ (Mott law) or 0.5 (Efros-Shklovskii law) [14] (Fig. 3). VRH stands for variable range hopping. In the Mott model, the localisation energy Δ is a function of temperature: $\Delta(T) = 1/4kT_0^{1/4}T^{3/4}$ [14]. The existence of Coulomb interactions giving rise to a correlation gap around the Fermi energy is taken into account in the Efros-Shklovskii model; then $\Delta(T) = 1/2kT_0^{1/2}T^{1/2}$.

In these concentration and temperature ranges, the $MR(H)$ varies less rapidly than the field, its magnitude is more or less constant below 20 K, and decreases above. As a function of Mn concentration, the MR under 8 T at $T = 10$ K increases in magnitude from -18% for $x = 0.35$ up to -29% for $x = 0.4$, then decreases (-24% for $x = 0.5$). In the range $0.35 \div 0.45$, the semiconducting-like behaviour is kept under fields up to 8 T. Figure 4 summarizes the MR amplitude observed in the series at 10 K under 4 T and 8 T. Note that for $x > 0.5$, the MR corresponds to a well ordered ferromagnetic state. Comparing with the variation of the resistivity in the series, we remark that the MR amplitude, which is a relative variation, follows that of the resistivity. A similar behaviour has been observed in the series of true semiconductors RNiSb (R = Tb, Dy, Ho) [15], and also in manganites [16,17].

In the temperature and concentration ranges where the resistivity can be fitted to a Mott law, the Mott temperature decreases under field, which means that the localisation energy is reduced by spin alignment, and the localisation energy Δ in the range 40–120 K varies almost linearly with field. Even below 20 K, where the localisation law is not well followed, the logarithm of resistivity continues to decrease linearly with the field. The rather large MR amplitude observed in the localisation region and the lowering of the Mott temperature under field shows that the magnetic disorder is responsible for a large part – difficult to evaluate as the extrapolation to higher fields is not precise enough – of the resistivity, a factor which is particularly important for manganites [17].

Smaller MR values are observed for larger Mn concentrations, where the resistivity returns to a metallic regime and ferromagnetism occurs above room temperature, as the magnetic contribution is strongly reduced in the ordered range. For concentrations x(Mn) larger than 0.8, the low temperature MR is even positive, which corresponds to a ferromagnetic state with a quite high Curie temperature, weak spin disorder and possibly half metallic character.

2.2 $CoV_{1-x}Mn_xSb$ solutions

In stoichiometric CoVSb, the magnetoresistance is negative down to low temperatures (-1.4% at 2 K under 4 T). This may be understood as CoVSb is a weak itinerant ferromagnet with a low Curie point (from 11 to 23 K depending on sample), where spin fluctuations remain in the ordered range and are partly suppressed

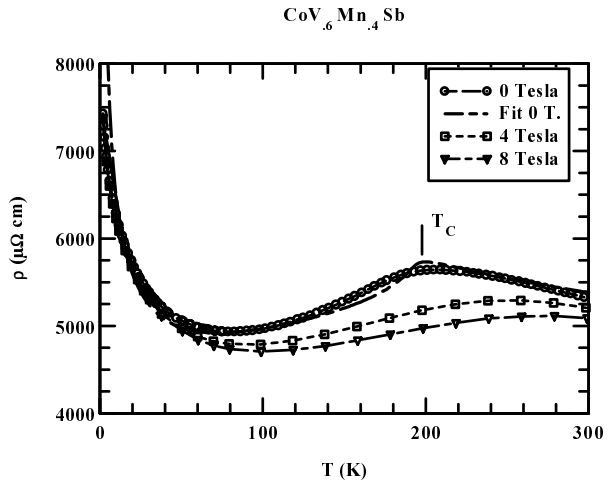

Fig. 5. Resistivity under 0, 4 and 8 T for $CoV_{0.6}Mn_{0.4}Sb$.

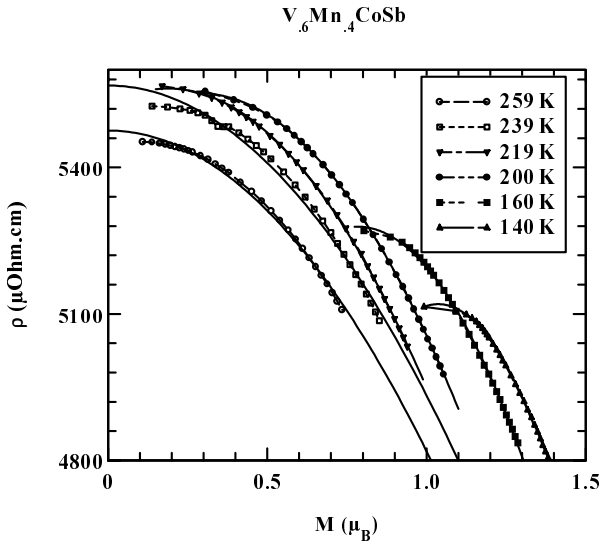

Fig. 6. Resistivity *versus* magnetization for $CoV_{0.6}Mn_{0.4}Sb$ around the Curie temperature.

by the applied field. For solutions with low Mn concentration ($x = 0.2 \div 0.25$), the Curie point rises up to 75–80 K, the resistivity has still a metallic behaviour and decreases below the Curie point, as in classical metallic ferromagnets [18]. The MR is positive and weak well below the Curie point. Turning now to the concentration range corresponding to the localisation regime, the resistivity behaviour has been analyzed previously for the $CoV_{0.6}Mn_{0.4}Sb$ solution [11] (Fig. 5); a similar behaviour is observed in the Mn concentration range from 0.3 to 0.5. The resistivity (Fig. 5) is semiconducting-like at low temperature, when the ferromagnetic magnetization is almost saturated; this behaviour is associated to the Anderson localisation of carriers by the atomic disorder between V and Mn, corresponding to a difference $\Delta Z = 2$ between nuclear charges. The localisation energy is smaller than in the case of Ti-Mn solutions ($\Delta Z = 3$). When increasing the temperature, ρ increases for $x = 0.4$ in the range from 80 K up to the Curie point ($T_C = 200$ K), due to the increase in spin disorder. Finally ρ decreases with increasing temperature above T_C or is almost constant, which is attributed to the localisation by both atomic and magnetic disorders in the paramagnetic range; the Mott temperature T_0, when it can be obtained in the paramagnetic range, is then larger than in the low temperature ferromagnetic range, which means that magnetic disorder plays an important role, as in the previous series.

Concerning the MR, it is small and positive at low temperature, when the magnetization is saturated and the resistivity decreases with temperature. It turns negative when the resistivity increases in the intermediate temperature range; its magnitude reaches a maximum near T_C, where the susceptibility is maximum, and decreases with temperature above T_C. This last behaviour is the classical one for the MR in ferromagnetic materials, as well for metallic systems [18] as for ferromagnetic manganites which undergo a metal-insulator transition [16,17].

Figure 6 shows the MR as a function of magnetization in the vicinity of the Curie point, together with fits to a parabolic variation. In the paramagnetic range,

$$[\rho(H) - \rho(0)]/\rho(0) = AM^2(H,\ T),$$

with $A = 0.17\ \mu_B^{-2}$ for the solid solution with $x = 0.4$.

The maximum MR amplitudes, recorded near the Curie point under 8 T, are respectively: 5.7% for $x = 0.3$ at 100 K, 10% for $x = 0.35$ at 100 K, 12% for $x = 0.4$ at $T_C = 200$ K, and 4% for $x = 0.5$ near $T_C = 290$ K. As for the previous series, we remark that the MR amplitude reaches its maximum in the range where localisation occurs. However, a comparison between the resistivity magnitudes at a given temperature is not straightforward, due to the large variation of magnetization in this concentration range. The MR amplitude remains quite large for high temperatures due to the enhancement of the susceptibility by ferromagnetic interactions just above the Curie point. However, it does not reach so high values as in the Ni(Ti, Mn)Sb series at low temperatures, and is much smaller than for ferromagnetic manganites.

In the ferromagnetic state of the present compounds, the MR varies as:

$$[\rho(H) - \rho(0)]/\rho(0) = A(T)[M(H,T) - M_{sp}(T)]^2$$

where $A(T)$ increases with decreasing temperature (Fig. 6). Due to the increasing spontaneous magnetization M_{sp}, the MR amplitude nevertheless decreases at low temperatures.

The resistivity behaviour could be nicely described by the localisation model [11]. The localisation energy Δ, difference between the mobility edge E_m and the Fermi energy E_F is expected to vary with the magnetic splitting of the subbands, thus with the magnetization: $E_m - E_F = \Delta 0 - \lambda M(H,T)$ [19]. However, problems were encountered when fitting the MR, as the calculated value was too high, and when trying to describe the quadratic variation of the MR as a function of field in the paramagnetic range.

One key of this problem may be the following: when the magnetization is large enough, only one spin direction (up-spin for instance) efficiently contributes to the transport, as the localisation energy is reduced for this spin direction. Conversely, in the paramagnetic state or close to T_C, we have to consider both spin directions [15]. We then assume that the resistivity is given by a localisation law where, for up-spin electrons, $\Delta_\uparrow = \Delta_0(1 - \lambda m)$, whereas for down-spin, $\Delta_\downarrow = \Delta_0(1 + \lambda m)$, where $m = M(H,T)/M_{sp}(T = 0)$ is the reduced magnetization. Such behaviour seems logical if the localisation is mainly due to magnetic disorder. The transport in parallel by the two spin subbands leads to a conductivity which can be expressed by: $\sigma(H,T) = \sigma(H = 0,T)\cosh(\lambda\Delta_0 m/kT)$, where cosh( ) is the hyperbolic cosine. As a consequence, the MR becomes a quadratic function of the magnetization (or field) in the paramagnetic state, as it is really for low fields; conversely it varies initially linearly with the field in the ferromagnetic range as there is a spontaneous magnetization, but its amplitude is lower than that calculated for only one spin direction. In the paramagnetic range, MR is proportional to $1/2(\lambda\Delta_0 m/kT)^2$, thus the ratio A is expected to depend on (Δ_0/kT), that is on the logarithm of the resistivity itself. A physical explanation for the increase in MR ratio in systems with a low carrier density was given by Majumdar and Littlewood, based on the variation of the magnetic correlation length with the carrier density [20].

There are some analogies with the giant MR encountered in RNiSb semiconductors (R = Tb, Dy, Ho) [15], which remain paramagnetic down to low temperatures: it has been shown that the MR amplitude scales as M^2, but again the ratio $A = MR/M^2$ varies more or less as the logarithm of the resistivity. A difference is that for rare earth compounds, the $4f$ shell is very localised and $4f$ moments are weakly coupled with the current carriers.

Finally, in the very low temperature range (below 4 K), non-ohmic behaviour has been observed on the current-voltage characteristics for the most localised phases, with anomalies for voltages ranging from a few to about 30 mV. It is difficult to separate this behaviour from the resistivity change due to Joule heating in the samples; thus we do not insist here on this phenomenon, although it may indicate the presence of a narrow Coulomb gap near the Fermi energy in line with the semiconducting-like behaviour at low temperatures.

3 Hall effect

The Hall effect was measured in the Van der Pauw geometry on square platelets 4×4 mm in surface with a thickness e smaller than 1mm, under fields varying between −4 to 4 T. The Hall signal is defined as $[V(H)-V(-H)]/2Ie$, the field reversal allowing to suppress the contribution of electrodes misalignment and that of the magnetoresistance. For magnetic samples, the Hall signal contains an anomalous term in addition to the normal one:

$$V/Ie = R_H^0 B_i + R_H^a M(H,\ T),$$

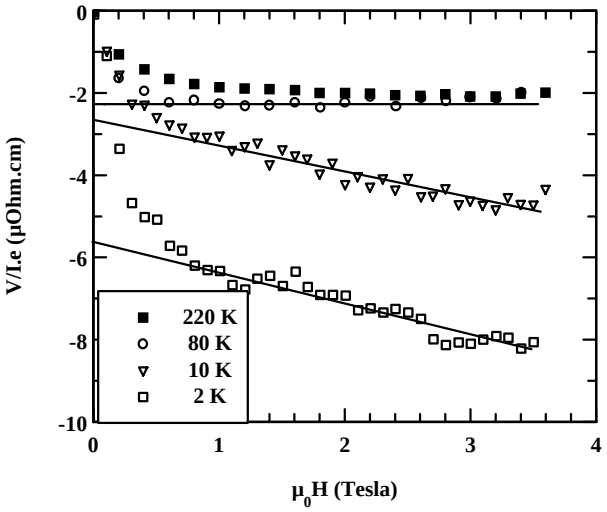

Fig. 7. Hall effect at a few temperatures for $CoV_{0.65}Mn_{0.35}Sb$.

where the internal field $B_i = H - n_d M$ contains the demagnetizing field term.

The Hall effect for NiMnSb was first measured by Otto *et al.* [21] and remeasured more recently [13]. The (positive) normal Hall coefficient R_H^0 is almost constant ($+0.12 \times 10^{-10}$ Ω m/T from [21], 0.11×10^{-10} from [13]) between 120 and 300 K, but rises at lower temperatures and reaches 0.4×10^{-10} Ω m/T near 4 K. The anomalous coefficient R_H^a increases with temperature from 100 K up to T_C, due to its relations with the resistivity through the skew scattering and side jump mechanisms [21]. However Hordequin *et al.* [13] observed that this term also becomes larger at lower temperatures, and $R_H^a M_{sp}$ reaches 0.065×10^{-10} Ω m at 4 K. These upturns below 100 K were attributed to the onset of the half metallic regime, which on one hand leads to the disappearance of an electron spin-down pocket, while on the other hand the carrier spin flip scattering is forbidden, which increases their mobility.

The Hall effect for the weak CoVSb ferromagnet has also been measured [22]. R_H^0 is negative below 200 K (about -5×10^{-10} Ωm/T), whereas a positive R_H^a arises below the Curie point; $R_H^a M_{sp}$ reaches 1.3×10^{-10} Ω m at helium temperature. Thus the anomalous and normal Hall coefficients have the same sign in NiMnSb, but opposite signs for CoVSb.

A few measurements have been performed for solid solutions with localisation. For $CoV_{0.65}Mn_{0.35}Sb$, the dominant term is the anomalous one, which evolves rapidly from -5.6×10^{-8} Ω m at 1.5 K to about -2.3×10^{-8} Ω m at 20 K (Fig. 7). The amplitude decrease is more gradual at higher temperatures, and the anomalous term is revealed up to room temperature by a strong curvature of the Hall signal. This term hides nearly completely the normal Hall effect, except below 10 K where both terms have the same sign. The order of magnitude of R_H^0 is then -4×10^{-10} Ω m/T at 10 K.

For $NiTi_{0.65}Mn_{0.35}Sb$, R_H^0 is about -10×10^{-10} Ω m/T for temperatures lower than 10 K, and about -12×10^{-10} Ω m/T for temperatures above 100 K. Between

these temperatures, an additional negative anomalous term due to the large susceptibility prevents the determination of R_H^0. Below 10 K, a non vanishing term $R_H^a M_{sp} = -0.23 \times 10^{-8}\ \Omega\,m$ is obtained by extrapolation to zero field, this anomalous term being attributed to a remanent magnetization of the spin glass state.

The values for R_H^0 are of the order of that found for CoVSb, whereas the magnitude of the resistivity is larger by about three orders of magnitude. Assuming one type of dominant carriers, their density n should be comparable to that for CoVSb, whereas the Hall mobility $\mu = R_H/\rho$ should be strongly reduced. A direct comparison of the Hall effect and the resistivity: $\rho = 5 \times 10^{-5}\ \Omega\,m$ and $R_H^0 = -4 \times 10^{-10}\ \Omega\,m/T$ for $CoV_{0.65}Mn_{0.35}Sb$, would give, again assuming a single band model, a density n of the order of 3 carriers by cell (4 formula units) and a low Hall mobility $\mu = 0.8 \times 10^{-5}$ m/s/V/m in the temperature range 50–200 K.

For $NiTi_{0.65}Mn_{0.35}Sb$ at 200 K, where $\rho = 6.15 \times 10^{-6}\ \Omega\,m$, it would gives $n = 1.3$ carrier/cell and $\mu = 1.6 \times 10^{-4}$ m/s/V/m. These calculations must be taken with much care, due to the different sheets of the Fermi surface and to the oversimplification of the model. We may suspect for instance a high degree of compensation in $CoV_{0.65}Mn_{0.35}Sb$ where R_H^0 is very small. Nevertheless, these crude data are coherent with the picture of Anderson localisation in these solutions: the density of states is still significant at the Fermi level, but this level lies below some mobility edge E_m giving rise to variable range hopping and to a very low mobility. Unfortunately no specific heat measurements, which would supply directly the magnitude of the density of states, are available at present on these phases. Let us note that, for $CoV_{0.65}Mn_{0.35}Sb$, the parameter $R_H^a M_{sp}$ rises quite rapidly at low temperature and reaches $-5.6 \times 10^{-8}\ \Omega\,m$ at 1.5 K, a value which is much larger than in CoVSb or NiMnSb. The anomalous Hall effect is related to the resistivity through side jump and skew scattering mechanisms. Its evolution at low temperature in the solid solution may be perhaps understood, together with the resistivity behaviour, by the onset of a kind of Efros-Shklovskii gap near the Fermi level [14,23].

4 Thermopower

The Seebeck coefficient S *versus* copper was measured by direct comparison to that of a known Cu/constantan thermocouple. Experiments were performed from 10 to 300 K for NiMnSb, but restricted to room temperature for other compounds and solid solutions. For NiMnSb [13], S is weak and negative down to 50 K, then turns positive in the low temperature half metallic range, where the spin-down electron pocket disappears. This last feature agrees with the upturn observed in the Hall effect behaviour. Room temperature data for different phases are reported in Table 1. In the NiTiSb-NiMnSb series, only a few samples with suitable shape were studied. Starting with a weak positive value for NiTiSb, S increases significantly up to 41 V/K in $NiTi_{0.65}Mn_{0.35}Sb$ where localisation is observed. Then S decreases to a small negative values for larger Mn contents.

Similar trends are observed in the CoVSb-CoMnSb series. S starts from a positive value for CoVSb, which is quite large for a metallic sample: according to band calculations [6,22], the Fermi level falls into a range of rapidly increasing density of states (DOS). Indeed this compound is a weak ferromagnet, which indicates that the density just meets the Stoner criterion. In the solid solutions, the Seebeck coefficient increases in magnitude up to a maximum (about 100 μ V/K) for $x(Mn) = 0.35$ (we however observe an unexplained strong negative value for $x = 0.3$). For larger Mn contents, S turns to weak values (slightly negative for $x = 0.6$ and slightly positive for $x = 0.8$, 0.9).

We thus observe rather high thermopower values in the concentration range where localisation phenomena occur; this agrees with some theories, which even predict an almost divergent thermopower at the metal-insulator transition in classical semiconductors [24]. This phenomenon is related to the low mobility of carriers and to the rapid evolution of the density of states. One other experimental trend is that S is positive for low Mn concentrations up to the concentration range for localisation, and turns negative for higher Mn content. In a single band picture, it would correspond to dominant positive carriers at low x, and to dominant electrons for large x, which is opposite to the predictions of band calculations, which show an increasing DOS $n(E)$ at the Fermi level for low Mn concentrations, mainly due to Ti or V 3d states. However, such a crude picture is certainly not valid, because several bands cross the Fermi level, and lead to different types of orbits, including open ones. The mobility, which is strongly reduced for these localised carriers, is probably the most significant factor, and is probably very different for Mn, V/Ti 3d electrons and those from other components.

Similarly the signs of Hall effect and thermopower do not agree even for the ending stoichiometric compounds: the normal R_H^0 coefficient is negative for CoVSb, whereas S is positive. The opposite behaviour is observed for NiMnSb (except below 50 K). Thus a deeper analysis should take care of the different bands and of the sign and mobility of carriers.

In the case where an Efros-Skhlovskii gap [14,23] would be present in the localised systems, this gap or pseudo-gap pinned at E_F for the electron concentration around the maximum of localisation would reinforce the minimum in DOS predicted by KKR/CPA calculations. This may enhance the thermopower, also explaining the maximum amplitudes observed in these concentration ranges. It is however not obvious to predict how the minimum in DOS will be displaced relatively to Fermi energy with the change in electron concentration around the localisation range, thus to estimate the sign of the derivative of the density of states due to this gap.

Unfortunately the large thermopower encountered in these solid solutions cannot be useful in practice, as the figure of merit and the power factor are much reduced due to the high electrical resistivity. Conversely, the atomic

Table 1. Curie (or spin glass) temperature, resistivity and Seebeck coefficient at room temperature for some phases.

Compound	T_C, T_{SG} (K)	ρ (300 K) ($\mu\Omega$.cm)	S (300 K) (μV/K)
NiTiSb	—	105	9
$NiTi_{0.65}Mn_{0.35}Sb$	$T_{SG} = 11$	5500	41
$NiTi_{0.6}Mn_{0.4}Sb$	12	3600	12
$NiTi_{0.2}Mn_{0.8}Sb$	$T_C = 580$	650	0
NiMnSb	730	25	−4
CoVSb [11]	10.5−23	350	43/47
$CoV_{0.75}Mn_{0.25}Sb$	75	600	58
$CoV_{0.7}Mn_{0.3}Sb$	75	3300	−64
$CoV_{0.65}Mn_{0.35}Sb$	82	5000	101/97
$CoV_{0.55}Mn_{0.45}Sb$	270	4500	−26
$CoV_{0.4}Mn_{0.6}Sb$	410	850	−4
$CoV_{0.3}Mn_{0.7}Sb$	482	450	2
$CoV_{0.2}Mn_{0.8}Sb$	487	550	3.5

disorder should reduce the thermal conductivity, which is favorable.

5 Comparison with band calculations

Can some conclusions be derived concerning effective masses, mobilities, and correlation lengths from a comparison of the above results with the band calculations? Hanssen and Mijnarends [2] give a description of the Fermi surface for NiMnSb at 0 K, which consist of three sheets of majority-spin bands. The 12th band corresponds to a hole pocket, the 13th and 14th bands correspond to open sheets with dominant hole character, but with parts of electron character. Above 80 K, it is likely that NiMnSb becomes a normal ferromagnetic metal [13], and a minority electron pocket becomes occupied around X point in the Brillouin zone, giving rise to the sign reversal in the thermopower and the strong drop in the normal Hall coefficient [13]. These last features may indicate that the mobility is higher for these electrons than for hole pockets, despite the fact that their effective mass can be larger due to the flatness of the band.

It is even more difficult to discuss about effective masses and mobilities in different bands for disordered solutions. Only band calculations for ordered superstructures would give information about them, but the band structures should be much more complex than for NiMnSb itself.

Nevertheless, the CPA gives an estimate of the total density of states at the Fermi level, although it neglects correlation effects or the existence of a Coulomb gap. The total DOS $N(E_F)$ at the Fermi level for two spin directions evolves from 40 states/Ry formula unit (NiTiSb) through 15.5 ($NiTi_{0.65}Mn_{0.35}Sb$) to 9.3 (NiMnSb), and from 60 states/Ry (CoVSb) to 13 ($CoV_{0.65}Mn_{0.35}Sb$). The density $N(E_F)$ is thus large in the localised range as revealed by the magnitude of the Hall effect. An estimate of the localisation length ξ can be obtained from these values and those of the Mott temperatures [11], according to the relation [25]:

$$kT_0 = 18/N(E_F)\xi^3.$$

For $NiTi_{0.65}Mn_{0.35}Sb$, $kT_0 = 0.207$ eV and $N(E_F) = 2.22 \times 10^{28}$ states/eV m^3 give $\xi = 16$ Å, whereas for $CoV_{0.65}Mn_{0.35}Sb$, $kT_0 = 0.027$ eV and $N(E_F) = 1.86 \times 10^{28}$ states/eV m^3 give $\xi = 33$ Å. These values being respectively 2.7 and 5.6 times the lattice parameter are reasonable and correspond to weak localisation.

6 Electron spin resonance

The electron spin resonance (ESR) of some $CoV_{1-x}Mn_xSb$ phases ($x = 0.2$, 0.25, 0.3, 0.35) was studied between 100 and 300 K using an X-band frequency of about 9 GHz with 100 kHz field modulation. In the paramagnetic range a single asymmetrical Lorentzian ESR line was observed. The absorption part of the resonance line was separated numerically from the total signal.

The g-factors are found between 1.98 and 2.007 and are independent of temperature within the limits of experimental errors. The linewidth DH increases almost linearly with temperature (Fig. 8). All these pictures are expected for ESR on localised spins in metals. The localised spins are manganese magnetic moments, but it is difficult to say which is the ground-state spin configuration. It is clear that the observed signal cannot be attributed to isolated Mn^{2+}, Mn^{3+} or Mn^{4+} ions as in fully ionic compounds.

The temperature broadening of the linewidth $b = d(DH)/dT$ is strongly dependent on the Mn concentration: the "b" value decreases from about 17 Oe/K for $x = 0.2$ to 2.2 Oe/K for 0.3 and is smaller than 1 Oe/K for $x = 0.35$. Such behaviour can be attributed to strong "bottleneck effect" for ESR of localised moments, which are coupled *via* conduction electrons by the indirect exchange interactions [26]. The bottleneck may be opened by a decrease

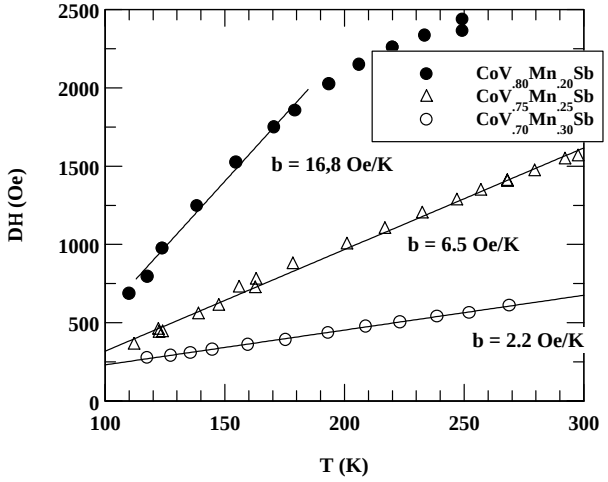

Fig. 8. ESR linewidth for three samples in the $CoV_{1-x}Mn_xSb$ series.

in Mn concentration. A quantitative discussion of this effect is not possible at the present state of the study. Due to the bottleneck regime it is almost impossible to discuss changes in the density of states. This ESR data only confirm the rather localised character of magnetic moments.

7 Conclusions

Peculiar phenomena were observed for phases where the previous study of resistivity revealed localisation phenomena, such as large values of the magnetoresistance and thermopower. These data reinforce the idea of Anderson localisation in these series. The behaviour of the resistivity and Hall effect for localised phases, which both strongly increase at low temperatures, may also support the existence of some narrow correlation gap in these systems. The interpretation of the signs observed for the Hall effect and thermopower is however not evident, carriers mobilities which are strongly reduced should play a large role.

We observed that the magnetoresistance to magnetization ratio $A = MR/M^2$ is larger for a stronger resistivity. A similar variation has been observed in mixed valent $La_{1-x}Sr_xMnO_3$ by Urushibara *et al.* [16], who showed that the ratio A increases as the localisation of carriers increases from $x = 0.4$ to $x = 0.2$. This could be explained within the frame of localisation picture, provided that the localisation energy comes mainly from the magnetic disorder, leading to an increase in MR ratio for large resistivities. In other words the change in the localisation energy under field (or magnetization) should be larger for a more localised system.

A comparison with manganites, where localisation phenomena are also present, is interesting. The situation is indeed rather different between these systems. First manganites are more ionic and the present compounds rather semi-covalent. The limiting pure compounds in manganites (La, Ca, Sr, Ba manganites) are antiferromagnetic insulators at 0 K. Thus the random potential due to doping is expected to be much less screened in manganites. Doping allows to explore completely the metal-insulator transition; in addition strong localisation effects linked to charge order also exist for rational "doping" concentrations (50–50 for instance). Conversely, in the present case, the limiting compounds are true metals and the solid solutions never display an insulating state at 0 K, as the extrapolated conductivity always remains finite. Thus the compounds are always on the metallic side, and localisation effects are much weaker in this case.

Second, only manganese occupies the corresponding site in manganites, the crystal electric field implies that t_{2g} electrons are rather localised, and coupled *via* a strong intraatomic Hund energy to the current carriers coming from the hybridized states of e_g electrons [16,17]. Hopping or localisation are thus function of the relative orientation of moments, as the Hund coupling prevents hopping between antiparallel moments. Conversely, there is substitutional disorder on the Mn site in the present alloys, Mn nearest neighbours are randomly disordered, thus the relative orientation of moments (magnetisation) plays a weaker role. This may explain the weaker magnetoresistance effects in the present compounds.

Some compounds in the $NiTi_{1-x}Mn_xSb$ series were elaborated in University I. Franko (Lviv, Ukraine) by L.P. Romaka and R.V. Skolozdra.

References

1. R.A. de Groot, F.M. Mueller, P.G. van Engen, K.H.J. Buschow, Phys. Rev. Lett. **50**, 2024 (1983).
2. K.E.H. Hanssen, P.E. Mijnarends, Phys. Rev. B **34**, 5009 (1986).
3. F.G. Aliev, V.V. Kozyrkov, V.V. Moshchakkov, R.V. Skolozdra, K. Durczewski, Z. Phys. B Cond. Matter **80**, 353 (1990); F.G. Aliev, Physica B **171**, 199 (1991).
4. M.A. Kouacou, J. Pierre, R.V. Skolozdra, J. Phys. Cond. Matter **7**, 7373 (1995).
5. S.J. Youn, B.I. Min, Phys. Rev. B **51**, 10436 (1995).
6. J. Tobola, J. Pierre, S. Kaprzyk, R.V. Skolozdra, M.A. Kouacou, J. Magn. Magn. Mater. **159**, 192 (1996); J. Phys. Cond. Matter **10**, 1 (1998); J. Tobola, J. Pierre, J. Alloys Comp. **296**, 243 (2000).
7. P.G. van Engen, K.H.J. Buschow, R. Jongebreur, M. Erman, Appl. Phys. Lett. **42**, 202 (1983).
8. K. Takanashi, M. Watanabe, H. Fujimori, J. Appl. Phys. **67**, 393 (1990).
9. C. Uher, J. Yang, S. Hu, D.T. Morelli, G.P. Meisner, Phys. Rev. B **59**, 8615 (1999); H. Hohl, A.P. Ramirez, C. Goldmann, G. Ernst, B. Wölfing, E. Bucher, J. Phys. Cond. Matter **11**, 1697 (1999).
10. S. Poon, T.M. Tritt, S. Bhattacharya, V. Ponnambalam, A.L. Pope, R.T. Littleton, V.M. Browning, *Proc. of Intern. Conf. on Thermoelectrics* (Baltimore, 1999).
11. K. Kaczmarska, J. Pierre, J. Tobola, R.V. Skolozdra, Phys. Rev. B **60**, 373 (1999).
12. A. Bansil, S. Kaprzyk, P.E. Mijnarends, J. Tobola, Phys. Rev. B **60**, 13396 (1999).

13. C. Hordequin, D. Ristoiu, L. Ranno, J. Pierre, Eur. Phys. J. B **16**, 287 (2000).
14. T.G. Castner, in *Hopping transport in solids*, edited by M. Pollack, B. Shklovskii (North Holland, Amsterdam, 1991).
15. J. Pierre, I. Karla, J. Magn. Magn. Mater. **217**, 74 (2000).
16. A. Urushibara, Y. Morimoto, T. Arima, A. Asamitsu, G. Kido, Y. Tokura, Phys. Rev. B **51**, 14103 (1995); Y. Tokura, Y. Tomioka, J. Magn. Magn. Mater. **200**, 1 (1999).
17. J.M.D. Coey, M. Viret, S. von Molnar, Adv. Phys. **48**, 167 (1999).
18. P.G. De Gennes, J. Friedel, J. Phys. Chem. Solids **4**, 71 (1958).
19. S. von Molnar, T. Penney, in *Physics of disordered materials* (Plenum, New York, 1985), Vol. 3, p. 183.
20. P. Majumdar, P. Littlewood, Phys. Rev. Lett. **81**, 1314 (1998).
21. M.J. Otto, H. Feil, R.A. van Woerden, J. Wijngaard, P.J. van der Valk, C.F. van Bruggen, C. Haas, J. Magn. Magn. Mater. **70**, 33 (1987); M.J. Otto, R.A.M. van Woerden, P.J. van der Valk, J. Wijngaard, C.F. van Bruggen, C. Haas, K.H.J. Buschow, J. Phys. Cond. Matter **1**, 2341 (1989).
22. J. Kaczmarska, J. Pierre, J. Beille, J. Tobola, R.V. Skolozdra, G.A. Melnik, J. Magn. Magn. Mater. **187**, 210 (1998).
23. C.M. Varma, Phys. Rev. B **54**, 7328 (1996).
24. K. Durczewski, A. Krzywicki, Phys. Rev. B **58**, 10302 (1998).
25. M. Viret, L. Ranno, J.M.D. Coey, Phys. Rev. B **55**, 8067 (1997).
26. S.E. Barnes, Adv. Phys. **30**, 801 (1981).